

# Gravity currents in a porous medium at an inclined plane

By **DOMINIC VELLA** AND **HERBERT E. HUPPERT**

Institute of Theoretical Geophysics, Department of Applied Mathematics and Theoretical Physics, University of Cambridge, Wilberforce Road, Cambridge, CB3 0WA, U. K.

(Received 20 October 2018)

We consider the release from a point source of relatively heavy fluid into a porous saturated medium above an impermeable slope. We consider the case where the volume of the resulting gravity current increases with time like  $t^\alpha$  and show that for  $\alpha < 3$ , at short times the current spreads axisymmetrically, with radius  $r \sim t^{(\alpha+1)/4}$ , while at long times it spreads predominantly downslope. In particular, for long times the downslope position of the current scales like  $t$  while the current extends a distance  $t^{\alpha/3}$  across the slope. For  $\alpha > 3$ , this situation is reversed with spreading occurring predominantly downslope for short times. The governing equations admit similarity solutions whose scaling behaviour we determine, with the full similarity form being evaluated by numerical computations of the governing partial differential equation. We find that the results of these analyses are in good quantitative agreement with a series of laboratory experiments. Finally, we discuss the implications of our work for the sequestration of carbon dioxide in aquifers with a sloping, impermeable cap.

---

## 1. Introduction

Horizontal differences in density between two fluids lead to the propagation of so-called gravity currents. These currents are of interest in a number of industrial as well as natural applications and so obtaining an understanding of the way in which they propagate is a subject that has motivated a considerable amount of current research (Huppert 2006).

In previous publications, our understanding of axisymmetric viscous gravity currents on an impermeable boundary (Huppert 1982) has been generalised to take account of the effects of a slope (Lister 1992) as well as the propagation of a current in a porous medium (Huppert & Woods 1995; Lyle *et al.* 2005). Here, we consider the propagation of a gravity current from a point source in a porous medium at an impermeable sloping boundary. Of particular interest is the evolution of the current away from the axisymmetric similarity solution found by Lyle *et al.* (2005).

We begin by deriving the evolution equations for the shape of a current whose volume varies in time like  $qt^\alpha$ . A scaling analysis of these governing equations reveals the extent of the current as a function of time up to a multiplicative constant. The full form of the similarity solutions that give rise to these scalings can only be determined by numerical means, however, and to do so we modify the numerical code of Lister (1992). For some particular values of  $\alpha$ , it is possible to make analytical progress; these cases are considered separately and provide a useful check of the numerical scheme. We then compare the results of the numerical calculations to a series of experiments and find good quantitative agreement between the two. Finally, in the last section, we discuss the implications of our

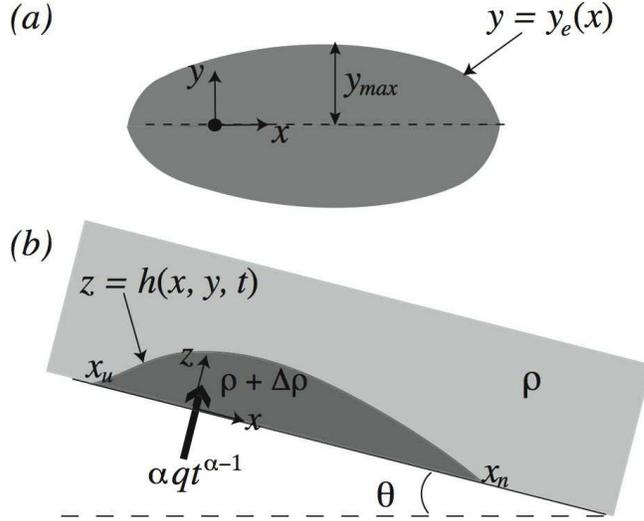


FIGURE 1. Sketches of a gravity current, of density  $\rho + \Delta\rho$ , propagating in a porous medium saturated with liquid of density  $\rho$  above an inclined plane. (a) Plan view of the current and (b) horizontal section through the current.

results in geological settings, with particular emphasis on the implications of our work for the sequestration of carbon dioxide.

## 2. Formulation

### 2.1. Governing equations

We consider a gravity current consisting of fluid material of density  $\rho + \Delta\rho$  in a deep porous medium saturated with fluid of density  $\rho$ , which is bounded by an impermeable barrier at an angle  $\theta$  to the horizontal (see figure 1 for a sketch of the setup). That the saturated porous medium is deep in comparison with the vertical extent of the current allows us to neglect the motion of the surrounding fluid, simplifying the problem considerably. We use the natural Cartesian co-ordinate system centred on the mass source and aligned with the slope of the impermeable boundary. The depth,  $h(x, y, t)$ , of the gravity current is then determined by continuity combined with Darcy's law (see Bear 1988, for example) and the assumption that the pressure in the current is hydrostatic, i.e.

$$P - P_0 = \Delta\rho gh \cos\theta - (\rho + \Delta\rho)gz \cos\theta + \rho gx \sin\theta \quad (z < h), \quad (2.1)$$

with  $P_0$  constant. Here, Darcy's law takes the form

$$\mathbf{u} = -\frac{k}{\mu} [\nabla P - (\rho + \Delta\rho)g(\sin\theta, 0, -\cos\theta)], \quad (2.2)$$

where  $k$  is the permeability of the porous medium and  $\mu$  is the viscosity of the liquid. The velocity within the porous medium is therefore given by

$$\mathbf{u} = -\frac{k\Delta\rho g}{\mu} \left( -\sin\theta + \cos\theta \frac{\partial h}{\partial x}, \cos\theta \frac{\partial h}{\partial y}, 0 \right). \quad (2.3)$$

Using this along with the conservation of mass, we obtain

$$\frac{\partial h}{\partial t} = \frac{k\rho g'}{\mu\phi} \left( \frac{\cos\theta}{2} \nabla^2 h^2 - \sin\theta \frac{\partial h}{\partial x} \right), \quad (2.4)$$

where  $\phi$  is the porosity of the porous medium and  $g' \equiv g\Delta\rho/\rho$ . Equation (2.4) is a nonlinear advection–diffusion equation for the current thickness, with the two terms on the right hand side representing the gravity–driven spreading of the current and its advection downslope, respectively.

It is common to close the system by requiring that the volume of the current depend on time like  $qt^\alpha$  for some constant  $\alpha \geq 0$  (Huppert 1982; Lister 1992; Huppert & Woods 1995). This constraint leads to solutions of self-similar form (as we shall see again in this case) but also covers the natural cases of a fixed volume release ( $\alpha = 0$ ) and a constant flux release ( $\alpha = 1$ ). To impose this volume constraint, (2.4) must be solved along with

$$\phi \int_{x_u}^{x_n} \int_{-y_e(x)}^{y_e(x)} h \, dy \, dx = qt^\alpha, \quad (2.5)$$

with  $|y| = y_e(x)$  giving the edge of the current for  $x_u(t) < x < x_n(t)$ . Note that (2.5) contains an extra multiplicative factor of  $\phi$ , which was omitted in the study of an axisymmetric current in a porous medium by Lyle *et al.* (2005).

Equations (2.4) and (2.5) may be non-dimensionalized by setting  $T = t/t^*$ ,  $H = h/h^*$ ,  $X = x/x^*$  and  $Y = y/y^*$ , where

$$t^* \equiv \left( \frac{q}{\phi V^3 \tan \theta} \right)^{\frac{1}{3-\alpha}}, \quad x^* = y^* \equiv Vt^*, \quad h^* \equiv x^* \tan \theta, \quad (2.6)$$

and

$$V \equiv \frac{k\rho g' \sin \theta}{\mu\phi} \quad (2.7)$$

is the natural velocity scale in the problem. In non-dimensional terms, therefore, the current satisfies

$$\frac{\partial H}{\partial T} = \nabla \cdot (H\nabla H) - \frac{\partial H}{\partial X}, \quad (2.8)$$

along with the volume conservation constraint

$$\int_{X_u}^{X_n} \int_{-Y_e(X)}^{Y_e(X)} H \, dY \, dX = T^\alpha. \quad (2.9)$$

## 2.2. Scalings

To aid our physical understanding of the spreading of the gravity current, we begin by considering the scaling behaviour of the spreading in the limits of short and long times. For  $\alpha < 3$ , (2.3) shows that at short times ( $T \ll 1$ ) the typical horizontal velocity scale is  $X/T \sim H/X$  so that  $H \sim X^2/T$ . Further,  $X \sim Y$  and volume conservation (2.9) requires that  $HXY \sim T^\alpha$ . From this we therefore find the axisymmetric scalings obtained by Lyle *et al.* (2005), namely

$$H \sim T^{\frac{\alpha-1}{2}}, \quad X \sim Y \sim T^{\frac{\alpha+1}{4}}. \quad (2.10)$$

At long times ( $T \gg 1$ ), again for  $\alpha < 3$ , the typical downslope velocity of the current is  $X/T \sim 1$  while in the across-slope direction we have  $Y/T \sim H/Y$ . Combined with volume conservation  $XYH \sim T^\alpha$  these scalings lead to

$$H \sim T^{\frac{2\alpha-3}{3}}, \quad X \sim T, \quad Y \sim T^{\frac{\alpha}{3}}, \quad (2.11)$$

so that the current spreads predominantly downslope. It is worth noting here that the long time scaling  $X \sim T$  is unsurprising because (2.8) may be simplified by moving into a frame moving at unit speed downslope (Huppert & Woods 1995). We also note that

Regime	Downslope extent $x$	Cross-slope extent $y$	Thickness $h$
$\alpha < 3 \quad t \ll t^*$	$\sim \left(\frac{Vq}{\phi \tan \theta}\right)^{1/4} t^{(\alpha+1)/4}$	$\sim \left(\frac{Vq}{\phi \tan \theta}\right)^{1/4} t^{(\alpha+1)/4}$	$\sim \left(\frac{q \tan \theta}{\phi V}\right)^{1/2} t^{(\alpha-1)/2}$
$\alpha < 3 \quad t \gg t^*$	$\sim Vt$	$\sim \left(\frac{q}{\phi \tan \theta}\right)^{1/3} t^{\alpha/3}$	$\sim \left(\frac{q^2 \tan \theta}{\phi^2 V^3}\right)^{1/3} t^{(2\alpha-3)/3}$
$\alpha > 3 \quad t \ll t^*$	$\sim Vt$	$\sim \left(\frac{q}{\phi \tan \theta}\right)^{1/3} t^{\alpha/3}$	$\sim \left(\frac{q^2 \tan \theta}{\phi^2 V^3}\right)^{1/3} t^{(2\alpha-3)/3}$
$\alpha > 3 \quad t \gg t^*$	$\sim \left(\frac{Vq}{\phi \tan \theta}\right)^{1/4} t^{(\alpha+1)/4}$	$\sim \left(\frac{Vq}{\phi \tan \theta}\right)^{1/4} t^{(\alpha+1)/4}$	$\sim \left(\frac{q \tan \theta}{\phi V}\right)^{1/2} t^{(\alpha-1)/2}$

TABLE 1. Summary of the asymptotic scalings for the dimensions of a gravity current in a porous medium at an inclined plane. Here dimensional notation is used for clarity, and  $t^*$  and  $V$  are as defined in (2.6) and (2.7), respectively.

the scaling  $Y \sim T^{\alpha/3}$  is identical to that found by Lister (1992) for a viscous current on a slope.

When  $\alpha > 3$ , the importance of the two downslope terms (the diffusive and translational terms) reverses. In particular, at long times  $(HH_X)_X \gg H_X$ , so that we in fact recover the axisymmetric spreading scalings given in (2.10) as being relevant for  $T \gg 1$ . Conversely, for  $T \ll 1$  we recover the non-axisymmetric scalings of (2.11). A summary of the different scaling regimes expected is given in dimensional terms in table 1.

That we observe axisymmetric spreading if  $\alpha > 3$  and  $T \gg 1$  is surprising, but is a consequence of the fact that the downslope flux in a porous medium gravity current is only weakly dependent on the local height and so can be swamped by the spreading terms in (2.8). In the viscous case, this is not possible because the downslope flux is able to remove the incoming flux much more efficiently and penalizes the accumulation of material at a particular point more.

### 2.3. Numerics

The axisymmetric spreading of a gravity current in a porous medium above an horizontal plane was considered by Lyle *et al.* (2005). In particular, they determined the coefficients in the scalings (2.10) by finding a solution dependent on one similarity variable in this case. To determine the prefactors in the non-axisymmetric scaling relations (2.11), it is necessary to resort to numerical solutions of (2.8) and (2.9). The numerical code used to do this was adapted from that used by Lister (1992) for a viscous gravity current on an inclined plane, with minor alterations to make it applicable to a gravity current in a porous medium. This code is an implementation of a finite-difference scheme on a rectangular grid with time-stepping performed using an alternating-direction-implicit method. Equation (2.8) was written in flux-conservative form allowing the diffusive and advective terms to be represented by the  $\Pi$ 'in scheme (Clauser & Kiesner 1987). More details of the numerical scheme may be found in Lister (1992).

## 3. Special values of $\alpha$

In this section, we consider separately particular values of  $\alpha$  that are of special interest. In some of these cases, it is possible to make progress analytically providing useful checks on the numerical scheme discussed in section 2.3, but they also shed light on situations of practical interest.

### 3.1. Constant volume

As already noted, the differential equation in (2.8) may be simplified by moving into a frame translating at unit speed downslope. However, for general values of  $\alpha$ , this corresponds to a point source that is moving uphill in the new frame, complicating the analysis. For a current of constant volume,  $\alpha = 0$ , there is no distinguished source point and we let  $X' \equiv X - T$ . The resulting transformation of (2.8) has an axisymmetric similarity solution (Lyle *et al.* 2005), which may be written

$$H(X, Y, T) = \frac{1}{8T^{1/2}} \left( \frac{4}{\sqrt{\pi}} - \frac{R'^2}{T^{1/2}} \right), \quad (3.1)$$

where  $R' \equiv (X'^2 + Y^2)^{1/2}$ .

### 3.2. Constant flux: A steady state

For very long times  $T \gg 1$ , we expect that a constant flux current (corresponding to  $\alpha = 1$ ) will approach a steady state, whose shape we now determine. We expect this steady shape to be observed far from the nose of the current, since the nose is always unsteady, requiring that  $X \ll T$ . Sufficiently far downstream from the source ( $X \gg 1$ ), the steady shape is given by

$$\frac{\partial^2 H^2}{\partial Y^2} = 2 \frac{\partial H}{\partial X}, \quad (3.2)$$

which has a similarity solution of the form  $H(X, Y) = X^{-1/3} f(Y/X^{1/3})$  where the function  $f$  satisfies

$$\frac{d^2 f^2}{d\eta^2} + \frac{2}{3} \left( f + \eta \frac{df}{d\eta} \right) = 0, \quad \int_{-\eta_e}^{\eta_e} f \, d\eta = 1, \quad f(\pm\eta_e) = 0. \quad (3.3)$$

This has solution

$$f(\eta) = \frac{1}{6} (\eta_e^2 - \eta^2), \quad (3.4)$$

where  $\eta_e = (9/2)^{1/3} \approx 1.651$  denotes the position of the current edge in similarity variables.

This shows that far away from the source and nose regions, we should expect the shape of unsteady currents to approach  $Y = (9X/2)^{1/3}$ . Superimposing this curve onto the numerically calculated current provides a useful check of the numerical scheme described in section 2.3. This comparison (see figure 2) shows that, away from both the nose and source regions, we do indeed see the steady state shape, though this region is confined to  $T^{-1} \ll X/T \ll 1$  in the rescaled co-ordinates used in figure 2.

It is interesting to note that the similarity solution (3.4) is precisely that given by Huppert & Woods (1995) for the shape of a two-dimensional current of constant volume spreading in a porous medium above an horizontal boundary. This correspondence arises because in the steady state case considered here, fluid moves downslope at a constant velocity — independently of its cross-slope position and the current height — so that  $X$  is a proxy for time. A material slice in the  $y$ - $z$  plane thus remains planar as it is advected downslope and so spreads laterally in exactly the same way that a fixed volume release does in two-dimensions.

### 3.3. $\alpha = 3$

When  $\alpha = 3$ , the non-dimensionalization leading to (2.8) breaks down because there is no longer a characteristic time-scale  $t^*$  of the motion. Instead, an additional natural velocity

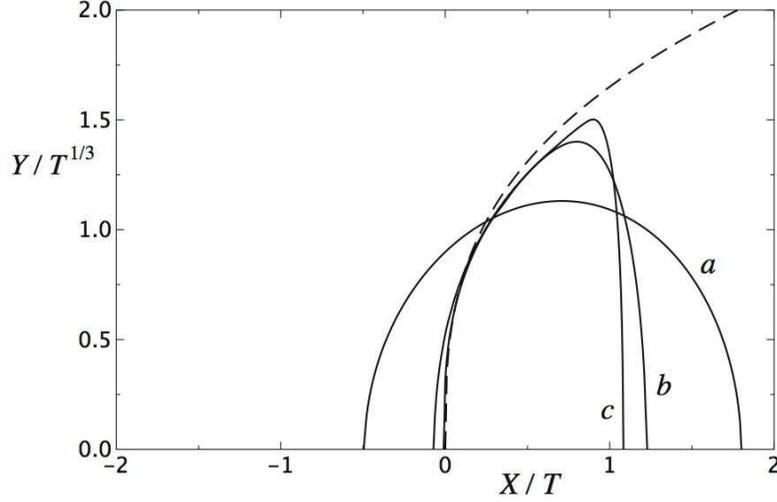


FIGURE 2. Numerical evolution of the boundary of the current in rescaled co-ordinates at (a)  $T = 1.23$ , (b)  $T = 9.52$  and (c)  $T = 270.9$ . The last of these is indistinguishable from the steady state shape that is found at long times in these rescaled variables. The similarity solution for the steady shape in the interior is given by  $Y = (9X/2)^{1/3}$  (dashed line) and is valid away from the source and the front regions, which in these rescaled variables requires that  $T^{-1} \ll X/T \ll 1$ .

scale,  $(q/\phi)^{1/3}$ , enters the problem. We thus define a new set of dimensionless variables  $\tilde{T} = t/\tilde{t}^*$ ,  $\tilde{H} = h/\tilde{h}^*$ ,  $\tilde{X} = x/\tilde{x}^*$  and  $\tilde{Y} = y/\tilde{y}^*$  where  $\tilde{t}^*$  is an arbitrary timescale and

$$\tilde{x}^* = \tilde{y}^* \equiv \left( \frac{q}{\phi \tan \theta} \right)^{1/3} \tilde{t}^*, \quad \tilde{h}^* \equiv \tilde{x}^* \tan \theta. \quad (3.5)$$

In these non-dimensional variables, the system becomes

$$\frac{\partial \tilde{H}}{\partial \tilde{T}} = \delta \left( \nabla \cdot (\tilde{H} \nabla \tilde{H}) - \frac{\partial \tilde{H}}{\partial \tilde{X}} \right), \quad (3.6)$$

along with volume conservation in the form

$$\int_{\tilde{X}_u}^{\tilde{X}_n} \int_{-\tilde{Y}_e(\tilde{X})}^{\tilde{Y}_e(\tilde{X})} \tilde{H} \, d\tilde{Y} \, d\tilde{X} = \tilde{T}^3, \quad (3.7)$$

where  $\delta \equiv V(\phi \tan \theta/q)^{1/3}$  is essentially the ratio of the two velocity scales in the problem. By substituting  $\tilde{H} = \tilde{T}\Phi(\xi, \eta)$  with  $\tilde{X} = \tilde{T}\xi$  and  $\tilde{Y} = \tilde{T}\eta$ , time can be eliminated from this problem completely so that  $\Phi$  is the solution of the two-dimensional problem

$$3\Phi = [\Phi(\xi + \delta(\Phi_\xi - 1))]_\xi + [\Phi(\delta\Phi_\eta + \eta)]_\eta, \quad (3.8)$$

(with subscripts denoting differentiation) and

$$\int_{\xi_u}^{\xi_n} \int_{-\eta_e}^{\eta_e} \Phi \, d\eta \, d\xi = 1. \quad (3.9)$$

The system (3.8) and (3.9) was solved by timestepping the problem in (3.6) and (3.7) using a minor modification of the code described in section 2.3. This was found to be a convenient method of solution and also demonstrates that time-dependent solutions

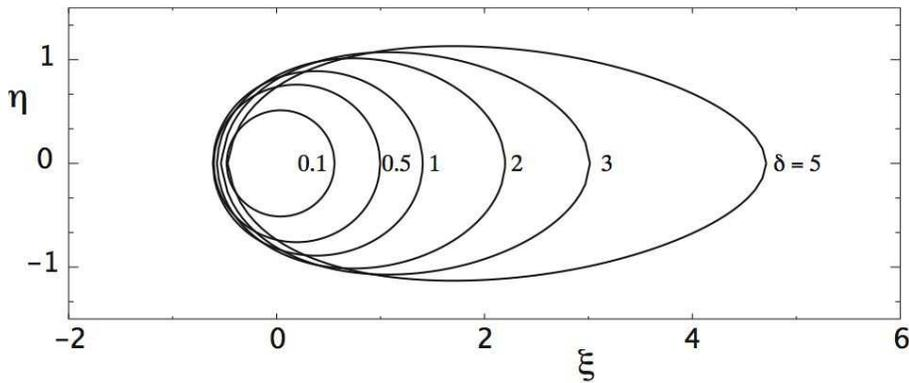


FIGURE 3. Numerical results showing the shape of currents with  $\alpha = 3$  obtained by solving (3.8) and (3.9) for six values of the parameter  $\delta$ . Labels refer to the value of  $\delta$  for each current.

converge on the time-independent solution. The results of this calculation are shown in figure 3 for a number of different values of  $\delta$ .

The importance of the case  $\alpha = 3$  as a transition between qualitatively different flow regimes is reminiscent of earlier work on gravity currents. For an axisymmetric gravity current, Huppert (1982) found that viscous forces dominate inertia at long times for  $\alpha < 3$  (being insignificant at short times) with the situation reversed for  $\alpha > 3$ . Acton *et al.* (2001) found that a viscous gravity current propagating over a permeable medium spreads only a finite distance if  $\alpha < 3$  but spreads indefinitely for  $\alpha > 3$ . Despite these similarities, the reappearance of a transition at  $\alpha = 3$  here is purely coincidental.

### 3.4. $\alpha > 3$

In section 2.2, we observed that for  $\alpha > 3$  a scaling analysis suggests that we should observe axisymmetric spreading for  $T \gg 1$ . For such values of  $\alpha$ , therefore, we expect to recover the axisymmetric solutions given by Lyle *et al.* (2005) in our numerical simulations. In particular, for  $\alpha = 4$  we would expect to find that

$$X_n, Y_{\max} \sim 0.8855T^{5/4},$$

where the prefactor here has been determined by repeating the analysis of Lyle *et al.* (2005). As shown in figure 4, this result is indeed obtained from our numerical results.

## 4. Experimental results

We conducted a series of experiments in which a saline solution (dyed red) was injected at constant flux ( $\alpha = 1$ ) into the base of a porous medium saturated with fresh water. The details of the experimental setup are as described by Lyle *et al.* (2005). In summary, the experiments were performed in a square-based Perspex tank of internal side length 61 cm and height 41 cm. The porous medium consisted of a self-supported matrix of Glass ballotini (diameter 3 mm), which filled the tank to a height of 25 cm. In contrast to the experiments of Lyle *et al.* (2005), the Perspex tank was tilted (so that the gravity current was propagating on a slope) and the saline solution was injected at the edge of the tank, away from the corner because the inherent symmetry is different here to that of the axisymmetric case. Video footage of the motion was captured using a CCD camera and measurements of the front distance down slope  $x_n$  as well as the maximum lateral

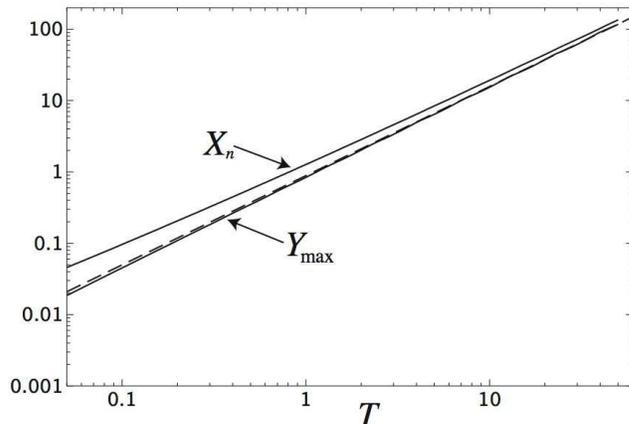


FIGURE 4. Numerical results for the positions of the current edge  $X_n$  and  $Y_{\max}$  as a function of time  $T$  for  $\alpha = 4$  (solid lines). For  $T \gg 1$  these obey the axisymmetric spreading relationship,  $X_n, Y_{\max} \sim 0.8855T^{5/4}$  (dashed line), that we expect from the axisymmetric analysis of Lyle *et al.* (2005).

<i>Expt.</i>	<i>Symbol</i>	$g'$ (cm s <sup>-2</sup> )	$q$ (cm <sup>3</sup> s <sup>-1</sup> )	$\theta$ (°)	$t^*$ (s)	$x^*$ (m)	$h^*$ (m)
1	△	91	2.14	9.5	40.5	0.112	0.019
2	□	99	1.31	10	25.2	0.080	0.014
3	◇	99	3.04	18	11.9	0.067	0.022
4	●	99	4	18	13.7	0.077	0.025
5	■	99	5.78	18	16.5	0.093	0.030
6	★	91	3.86	5	196.2	0.286	0.025

TABLE 2. Parameter values investigated in the six experiments presented here as well as the symbol used to represent their results in figure 5.

extent of the current  $y_{\max}$  were made using the image analysis software ImageJ†. The details of the six different values of  $g'$ ,  $q$  and  $\theta$  investigated are given in table 2, along with the relevant values of the typical scales  $t^*$ ,  $x^*$  and  $h^*$ . The latter estimates are based on the measurements of  $\phi = 0.37$  and  $k = 6.8 \times 10^{-9}$  m<sup>2</sup> given by Lyle *et al.* (2005). The experimental results of Lyle *et al.* (2005) are in very good agreement with theory once the additional factor of  $\phi$  in (2.5) is included. We therefore believe these values of  $\phi$  and  $k$  to be correct.

The experimental results plotted in figure 5 shows that the experimental results are in good agreement with the theoretical results produced by solving (2.8). The comparison between experimentally observed current profiles and those predicted from theoretical solutions of (2.8) shown in figure 6 is also favourable — particularly away from the source region. Two possible mechanisms may account for the slight discrepancy between experiments and theory observed: the drag exerted by the solid substrate on the current and the fact that the pore Reynolds number in our experiments is typically  $O(5)$ . Such a value of the pore Reynolds number suggests that we may be approaching the regime where Darcy’s law begins to break down, which is around  $Re = 10$  (Bear 1988).

† ImageJ is distributed by the National Institutes of Health and may be downloaded from: <http://rsb.info.nih.gov/ij/>

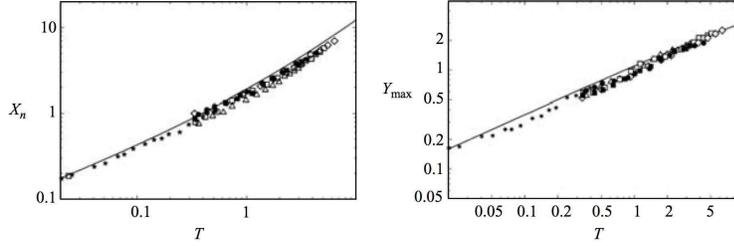


FIGURE 5. Numerical (solid line) and experimental (points) results for the position of the nose of the current,  $X_n$ , and the maximum horizontal extent of the current,  $Y_{\max}$ , as functions of time. The symbols used to represent each experimental run are given in table 2.

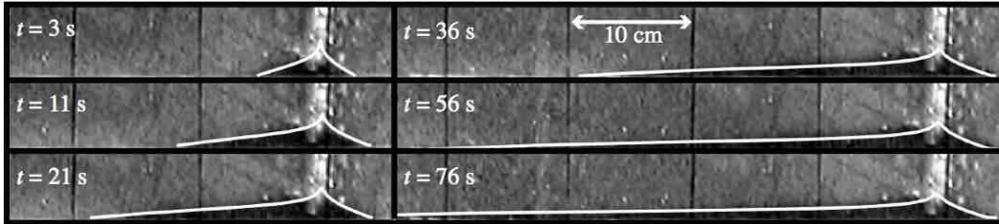


FIGURE 6. Comparison between the current profiles (dark) observed in Experiment 3 and those predicted by numerical computation (super-imposed white lines).

## 5. Geological relevance

Our experimental and numerical analyses have shown that shortly after the initiation of a constant flux gravity current ( $\alpha = 1$ ) it begins to spread axisymmetrically in the manner described by Lyle *et al.* (2005). However, at times much longer than the characteristic time  $t^*$  given in (2.6), the current loses its axisymmetry and propagates predominantly downslope. Since it propagates at constant velocity in this regime, the current propagates much further and faster in this case than would be the case if it remained axisymmetric. This is potentially problematic in a range of practical applications, such as the sequestration of carbon dioxide in which super-critical carbon dioxide is pumped into aquifers. Since the density of the liquid carbon dioxide lies in the range  $500 \pm 150 \text{ kgm}^{-3}$  (Chadwick *et al.* 2005), it remains buoyant with respect to the ambient water and so will rise up any inclined boundaries.

The time-scale,  $t^*$ , over which asymmetric spreading develops is of interest to those wishing to predict the course of the released current. While it is difficult to evaluate  $t^*$  in a precise manner because of the uncertainties in the properties of the surrounding rock, we can perform some estimates on the basis of the available data from the Sleipner field (Bickle *et al.* 2005; Chadwick *et al.* 2005). In this Norwegian field, around  $10^9 \text{ kg}$  of liquid  $\text{CO}_2$  is currently pumped into the local sandstone each year. Presumably due to geological complications, this single input flux is observed later to separate into around ten independent currents propagating within different horizons of the permeable layer, each of which has a volume flux lying in the region  $0.002 \lesssim q \lesssim 0.03 \text{ m}^3\text{s}^{-1}$ . Combined with typical measured values for the porosity and permeability of  $0.7 \leq k \leq 5 \times 10^{-12} \text{ m}^2$  and  $\phi = 0.31 \pm 0.04$  as well as the  $\text{CO}_2$  viscosity,  $\mu = 3.5 \pm 0.5 \times 10^{-5} \text{ Pas}$  (Bickle *et al.* 2005) we can estimate upper and lower bounds on the value of  $t^*$ . When  $\theta = 1^\circ$ , we find that  $0.03 \leq t^* \leq 14.2 \text{ years}$ . This suggests that the effects of non-axisymmetric spreading may indeed be important in the field. Because of the variety of values of the slope that we might expect to encounter in any geological setting, we note also that for  $\theta \ll 1$ ,

$t^* \sim \theta^{-4/(3-\alpha)}$ . For constant pumping rate ( $\alpha = 1$ ), this gives  $t^* \sim \theta^{-2}$ : i.e. the precise value of the timescale over which the current becomes asymmetric depends sensitively on  $\theta$ . This suggests that the different spreading regimes discussed here may be observed in the field and may also have practical implications.

Since injection occurs into confined layers of sediment, estimates for the vertical scale of the current,  $h^*$ , are also important. Interestingly,  $h^*$  is independent of  $\theta$  for  $\theta \ll 1$  (measured in radians) and  $\alpha = 1$  so that, with the parameter values given above, we find  $1.2 \leq h^* \leq 25$  m. This suggests that, near the source, the depth of the sediment layer may be similar to that of the current (and so exchange, confined flows may become significant). However, we expect that the scaling  $H \sim T^{-1/3}$  valid away from the source ensures that the present study will remain valid downstream.

We are grateful to John Lister for access to his code for a viscous current on a slope and to Robert Whittaker for discussions. Mike Bickle, Andy Chadwick, Paul Linden and John Lister also provided valuable feedback on an earlier draft of this paper.

#### REFERENCES

- ACTON, J. M., HUPPERT, H. E. & WORSTER, M. G. 2001 Two-dimensional viscous gravity currents flowing over a deep porous medium. *J. Fluid Mech.* **440**, 359–380.
- BEAR, J. 1988 *Dynamics of Fluids in Porous Media*. Dover.
- BICKLE, M., CHADWICK, A., HUPPERT, H. E., HALLWORTH, M. A. & LYLE, S. 2005 Modelling carbon-dioxide accumulation in the sleipner field: Implications for carbon sequestration (in preparation).
- BRADY, J. F. & KOCH, D. L. 1988 Dispersion in porous media. In *Disorder and Mixing* (ed. E. Guyon, J.-P. Nadal & Y. Pomeau), pp. 107–122. Kluwer.
- CHADWICK, R. A., ARTS, R. & EIKEN, O. 2005 4D seismic imaging of a CO<sub>2</sub> plume. In *Petroleum Geology: North-West Europe and Global Perspectives—Proceedings of the 6th Petroleum Geology Conference* (ed. A. G. Doré & B. A. Vining), pp. 1385–1399. The Geological Society, London.
- CLAUSER, C. & KIESNER, S. 1987 A conservative, unconditionally stable, second-order, three-point differencing scheme for the diffusion-convection equation. *Geophys. J. R. Astr. Soc.* **91**, 557–568.
- HUPPERT, H. E. 1982 The propagation of two-dimensional and axisymmetric viscous gravity currents over a rigid horizontal surface. *J. Fluid Mech.* **121**, 43–58.
- HUPPERT, H. E. 2006 Gravity currents: A personal perspective. *J. Fluid Mech.* (in press).
- HUPPERT, H. E. & WOODS, A. W. 1995 Gravity-driven flows in porous layers. *J. Fluid Mech.* **292**, 55–69.
- LISTER, J. R. 1992 Viscous flows down an inclined plane from point and line sources. *J. Fluid Mech.* **242**, 631–653.
- LYLE, S., HUPPERT, H. E., HALLWORTH, M. A., BICKLE, M. & CHADWICK, A. 2005 Axisymmetric gravity currents in a porous medium. *J. Fluid Mech.* **543**, 293–302.